

Signatures of Inelastic Scattering in Coulomb-Blockade Quantum Dots

T. Rupp, Y. Alhassid, and S. Malhotra
*Center for Theoretical Physics, Sloane Physics Laboratory,
Yale University, New Haven, Connecticut 06520*

We calculate the finite-temperature conductance peak–height distributions in Coulomb-blockade quantum dots in the limit where the inelastic scattering rate in the dot is large compared with the mean elastic tunneling rate. The relative reduction of the standard deviation of the peak-height distribution by a time-reversal symmetry-breaking magnetic field, which is essentially temperature-independent in the elastic limit, is enhanced by the inclusion of inelastic scattering at finite temperature. We suggest this quantity as an independent experimental probe for inelastic scattering in closed dots.

Quantum coherence of the electrons in ballistic quantum dots leads to distinct signatures in the mesoscopic fluctuations of their conductance [1]. These signatures are affected by decoherence and inelastic scattering of the electrons at finite temperature.

Various methods can be used to measure the dephasing rate of the electrons in open dots [2, 3]. In particular, the weak-localization effect (i.e., the reduction of the average conductance in the absence of a magnetic field) is sensitive to decoherence, and the suppression of this effect has been used to extract from experimental data the temperature dependence of the dephasing time.

In almost-isolated dots, the dephasing and inelastic scattering rates are expected to vanish at low excitations [4, 5]. It is, however, more difficult to determine experimentally the dephasing rate in such dots. An effect analogous to weak localization was predicted in the average Coulomb-blockade peak height of a closed (i.e., almost-isolated) chaotic dot [6, 7], and, in the limit of pure elastic scattering, was found to be essentially independent of temperature [7]. A recent experiment measured the weak-localization effect in closed dots and found good agreement with theory for temperatures kT below the mean level spacing Δ [8]. However, this effect was found to be suppressed for $kT \gtrsim \Delta$. Recently, the opposite limit where the mean inelastic scattering rate Γ_{in} is large compared with the mean elastic rate Γ_{el} [9] was studied, and the weak-localization effect in the average peak heights was found to be suppressed with increasing temperature [10]. This suppression was stronger than what was observed in the experiment, and it was concluded that the experimental data are consistent with $\Gamma_{\text{in}} \lesssim \Gamma_{\text{el}} \ll \Delta$. Ref. [11] has generalized the master-equations approach of Ref. [9] to study the effect of inelastic scattering on the average peak height in the crossover regime $\Gamma_{\text{in}} \sim \Gamma_{\text{el}}$. This allows one to determine from the data a mean inelastic scattering rate.

Here we study additional signatures of inelastic scattering on the conductance peak–height statistics in closed Coulomb-blockade quantum dots. We calculate the peak-height distributions at finite temperature in the inelastic limit $\Gamma_{\text{in}} \gg \Gamma_{\text{el}}$, and compare them with the corresponding distributions in the elastic limit. In particular, we

find that the decrease in the standard deviation of the conductance peak height upon application of a magnetic field (measured in units of the peak-height standard deviation in the presence of a magnetic field) is sensitive to inelastic scattering. This reduction in the standard deviation is temperature-independent in the elastic limit but is enhanced as a function of temperature in the inelastic limit, and therefore can be used as an experimental signature of inelastic scattering that is independent of the weak-localization suppression.

In Ref. [12], the ratio of the standard deviation of the peak height to its mean value was measured as a function of temperature in the presence of a magnetic field and compared with theory. It was found that the experimental values are suppressed in comparison with theoretical values calculated in the elastic limit [13], and the suppression is stronger at higher temperatures. To determine whether this suppression can be explained by inelastic scattering, we calculate the ratio of standard deviation to mean peak height in the inelastic limit. While we find some suppression (compared with the elastic limit), it is relatively small and insufficient to explain the observed data.

We consider a closed dot that is weakly coupled to the leads, where the average width Γ_{el} for elastic decay of an electron into the leads is much smaller than the mean spacing Δ of the single-particle levels in the dot. We also assume that the thermal energy kT is much smaller than the charging energy e^2/C , where C is the capacitance of the dot (Coulomb-blockade regime). To identify the effect of inelastic scattering of the electrons within the dot on the linear conductance, we compare two limits. In the elastic limit, the inelastic decay rate is assumed to be negligible compared with the elastic rate $\Gamma_{\text{in}} \ll \Gamma_{\text{el}}$, and an electron decays into one of the leads prior to any inelastic scattering event inside the dot. In the opposite limit of strong inelastic scattering, $\Gamma_{\text{in}} \gg \Gamma_{\text{el}}$, an electron tunneling into the dot has sufficient time to thermalize because of inelastic processes before leaving the dot.

Model. We further assume the limit $\Gamma_{\text{el}}, \Gamma_{\text{in}} < kT$ of sequential tunneling that can be described by a master-equations approach [9]. In the Coulomb-blockade regime, the conductance displays sharp peaks as a function of

gate voltage. The conductance G around a Coulomb-blockade peak can be written as

$$G(T, \tilde{E}_F) = \frac{e^2}{h} \frac{\pi \Gamma_{\text{el}}}{4kT} g(T, \tilde{E}_F), \quad (1)$$

where $g(T, \tilde{E}_F)$ is a dimensionless conductance at temperature kT and effective Fermi energy \tilde{E}_F (the latter can be tuned by varying the gate voltage). For $kT, \Delta \ll e^2/C$ and in the elastic limit, $g = g_{\text{el}}$ can be expressed as a sum of contributions from several levels λ in the dot [9]

$$g_{\text{el}} = \frac{2}{\Gamma_{\text{el}}} \sum_{\lambda} w_{\lambda} \frac{\Gamma_{\lambda}^{\text{l}} \Gamma_{\lambda}^{\text{r}}}{\Gamma_{\lambda}^{\text{l}} + \Gamma_{\lambda}^{\text{r}}}, \quad (2)$$

where $\Gamma_{\lambda}^{\text{l(r)}}$ is the partial elastic width of the level λ to decay to the left (right) lead, and $\Gamma_{\text{el}} = \overline{\Gamma_{\lambda}^{\text{l}} + \Gamma_{\lambda}^{\text{r}}}$. The contributions of the levels λ in Eq. (2) are weighted by factors

$$w_{\lambda} = 4f(\Delta F_N - \tilde{E}_F) \langle n_{\lambda} \rangle_N [1 - f(E_{\lambda} - \tilde{E}_F)], \quad (3)$$

which are a function of both T and \tilde{E}_F [13]. Here, f is the Fermi-Dirac distribution function, $\Delta F_N = F_N - F_{N-1}$, where F_N is the canonical free energy of N noninteracting particles, and $\langle n_{\lambda} \rangle_N$ are the canonical occupation numbers of the levels λ in the dot containing N electrons.

On the other hand, in the inelastic limit $\Gamma_{\text{in}} \gg \Gamma_{\text{el}}$, there is full thermalization of the electrons among the levels in the dot and $g = g_{\text{in}}$ with [9]

$$g_{\text{in}} = \frac{2}{\Gamma_{\text{el}}} \frac{(\sum_{\lambda} w_{\lambda} \Gamma_{\lambda}^{\text{l}}) (\sum_{\mu} w_{\mu} \Gamma_{\mu}^{\text{r}})}{\sum_{\nu} w_{\nu} (\Gamma_{\nu}^{\text{l}} + \Gamma_{\nu}^{\text{r}})}. \quad (4)$$

Note that the inelastic conductance (4) does not depend explicitly on Γ_{in} (in the inelastic limit).

In a chaotic dot (e.g., with irregular shape), the single-particle levels and wave functions follow random-matrix theory (RMT) statistics [1]. In particular, the partial elastic decay widths are fluctuating quantities that are independent and distributed according to a Porter-Thomas law $P_{\text{PT}}(\Gamma) \propto \Gamma^{\beta/2-1} \exp(-\beta\Gamma/\Gamma_{\text{el}})$, where the symmetry parameter β indicates the presence ($\beta = 1$) or absence ($\beta = 2$) of time-reversal symmetry. We assume that all levels have a common average partial width, i.e., $\overline{\Gamma_{\lambda}^{\text{l(r)}}} = \overline{\Gamma_{\mu}^{\text{l(r)}}$ for any pair of levels λ and μ , and that the leads are symmetric: $\overline{\Gamma_{\lambda}^{\text{l}}} = \overline{\Gamma_{\lambda}^{\text{r}}}$.

Method. We calculate the conductance peak-height distributions in the inelastic limit and compare them with the corresponding distributions in the elastic limit. In an RMT approach, we model the single-particle spectrum $\{E_{\lambda}\}$ of the quantum dot by the spectrum of a matrix that belongs to the corresponding Gaussian ensemble, i.e., the Gaussian orthogonal ensemble (GOE) for conserved time-reversal symmetry ($\beta = 1$), and the Gaussian unitary ensemble (GUE) for broken time-reversal

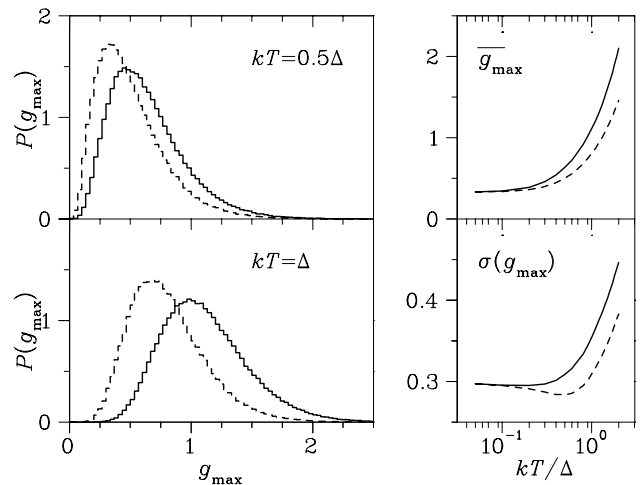


FIG. 1: Left panels: distribution $P(g_{\text{max}})$ of the dimensionless peak height g_{max} (see Eq. (1)) in the elastic (dashed lines) and inelastic (solid lines) limits at temperatures $kT = 0.5\Delta$ (top panel) and $kT = \Delta$ (bottom panel). Right panels: mean $\overline{g_{\text{max}}}$ (top) and standard deviation $\sigma(g_{\text{max}})$ (bottom) of the peak height g_{max} in the elastic (dashed lines) and inelastic (solid lines) limits.

symmetry ($\beta = 2$). The widths $\{\Gamma_{\lambda}^{\text{l}}; \Gamma_{\lambda}^{\text{r}}\}$ are taken as the squares of corresponding eigenvector components of the random matrix. For a given number N of electrons, both the canonical free energy F_N and the occupation numbers $\langle n_{\lambda} \rangle_N$ are calculated exactly using particle-number projection [13] (projecting from grand canonical partition functions with imaginary chemical potential). The elastic and inelastic conductance peaks at temperature T are then calculated as a function of the effective Fermi energy \tilde{E}_F from Eqs. (2) and (4), respectively. Finally, the height g_{max} of the corresponding conductance peak at temperature T is calculated by maximizing the function $g(T, \tilde{E}_F)$ with respect to \tilde{E}_F . The (numerical) distribution $P(g_{\text{max}})$ of the conductance peak heights is obtained by calculating the peak heights for an ensemble of RMT spectra and corresponding widths.

Results. We have carried out calculations for both non-degenerate and spin-degenerate single-particle spectra. In both cases Δ is the mean-level spacing per single-electron state (and is therefore half the orbital spacing in the spin-degenerate case). In the following, we assume non-degenerate energy levels unless otherwise stated.

Fig. 1 illustrates the temperature dependence of the distributions $P(g_{\text{max}})$ of conductance peak heights g_{max} in both the elastic and inelastic limits. In the left panels, the distributions $P(g_{\text{max}})$ are shown at temperatures of $kT = 0.5\Delta$ and Δ . In the right panels, the mean conductance peak height $\overline{g_{\text{max}}}$ and standard deviation $\sigma(g_{\text{max}})$ ($\sigma^2(g_{\text{max}}) = \overline{g_{\text{max}}^2} - \overline{g_{\text{max}}}^2$) are shown versus temperature kT . The elastic quantities are shown by dashed lines and the inelastic quantities by solid lines. All the

results in Fig. 1 are for the case of broken time-reversal symmetry ($\beta = 2$), but similar behavior is found for the case of conserved time-reversal symmetry ($\beta = 1$).

In the limit of $kT \ll \Delta$, only a single level λ contributes to the various sums in Eqs. (2) and (4) and $g_{\text{el}} = g_{\text{in}}$. In this limit, the distributions of the elastic and inelastic conductance coincide, and the mean peak height and its standard deviation take the analytically known GUE values for one-level conduction, $\overline{g_{\text{max}}} = 1/3$ and $\sigma(g_{\text{max}}) = 2\sqrt{5}/15 \approx 0.2981$ (the GOE values are $\overline{g_{\text{max}}} = 1/4$ and $\sigma(g_{\text{max}}) = \sqrt{2}/4 \approx 0.3536$). At finite temperatures, both the mean $\overline{g_{\text{max}}}$ and the standard deviation $\sigma(g_{\text{max}})$ are found to be enhanced by inclusion of inelastic scattering.

In recent work [8, 10], the finite-temperature suppression of the weak-localization effect in the average conductance peak height was suggested as a signature of inelastic scattering in the dot. Quantitatively, the weak-localization effect can be described by the increase of the average peak height upon breaking of time-reversal symmetry (relative to the GUE average value)

$$\alpha = 1 - \frac{\overline{g_{\text{max}}}^{\text{GOE}}}{\overline{g_{\text{max}}}^{\text{GUE}}} . \quad (5)$$

At low temperatures $kT \ll \Delta$, $\alpha = 0.25$ [6, 7]. In the elastic limit, α is fairly independent of temperature [7], as is shown by the open symbols in the lower panel of Fig. 2. The circles correspond to a non-degenerate single-particle spectrum and the diamonds to a spin-degenerate spectrum. As the temperature increases, more levels contribute to the elastic conductance but the ratio between the GOE and GUE averages of the peak height remains approximately constant, since the average over several contributing levels commutes with the ensemble average. A small suppression in the temperature range $kT/\Delta \lesssim 0.8$ is due to the suppressed occurrence of close lying levels in the GUE case, as pointed out already in Ref. [11]. Because level repulsion is stronger in the GUE than the GOE, the contribution of an excited level in the dot to the elastic conductance is smaller on average for the GUE, and α decreases somewhat.

On the other hand, inelastic scattering is found to reduce α at finite temperature and $\alpha \rightarrow 0$ for $kT \gg \Delta$. As a reminder, we show in the lower panel of Fig 2 the temperature dependence of α in the inelastic limit (solid symbols). While the data shown in Ref. [10] was obtained assuming equidistant levels, our results are calculated from RMT spectra yielding a stronger suppression of the inelastic α at low temperatures.

Here we suggest an independent signature of inelastic scattering that is experimentally accessible. We define γ as the reduction of the standard deviation of the conductance peak height (relative to the GUE standard deviation) when a time-reversal symmetry-breaking magnetic

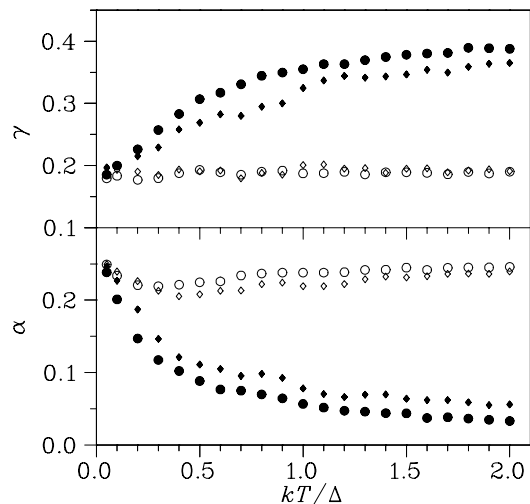


FIG. 2: The quantities γ (upper panel, Eq. (6)) and α (lower panel, Eq. (5)) versus temperature kT in the elastic (open circles) and inelastic (solid circles) limits. The diamonds are the corresponding results for a spin-degenerate spectrum. Notice the sensitivity of both γ and α to inelastic scattering.

field is applied,

$$\gamma = \frac{\sigma^{\text{GOE}}(g_{\text{max}})}{\sigma^{\text{GUE}}(g_{\text{max}})} - 1 . \quad (6)$$

In the upper panel of Fig. 2, we show γ versus temperature for both the elastic (open symbols) and inelastic (solid symbols) limits. For $kT \ll \Delta$, $\gamma = 3\sqrt{5}/(4\sqrt{2}) - 1 \approx 0.1859$, characteristic for conduction involving a single level in the dot. In the elastic limit, γ is essentially independent of temperature. However, at finite temperature, γ is sensitive to inelastic scattering. In the inelastic limit, γ increases from 0.1859 at $kT \ll \Delta$ to $\approx 0.42 \pm 0.01$ at $kT \gg \Delta$. The high temperature limit is obtained using the approximation $w_\lambda \approx w_\lambda^{(0)}/2$, where $w_\lambda^{(0)} = 1/\cosh^2[(E_\lambda - \tilde{E}_F)/2kT]$ are the thermal weights in the absence of charging energy [1].

The quantity γ can be calculated in the crossover regime $\Gamma_{\text{in}} \sim \Gamma_{\text{el}}$ using the generalized master-equations approach of Ref. [11]. It can therefore be used as an independent experimental probe from which the finite-temperature inelastic scattering rate can be determined.

Another dimensionless quantity of relevance to the experiments is the ratio between the standard deviation $\sigma(g_{\text{max}})$ and average $\overline{g_{\text{max}}}$ of the peak heights. This ratio was measured versus temperature in Ref. [12] and found to be significantly suppressed at higher temperatures in comparison with RMT calculations [13]. However, these predictions were based on the assumption of pure elastic scattering, and it was conjectured that the experimentally observed suppression might be due to inelastic scattering. Fig. 3 shows the temperature dependence of $\sigma(g_{\text{max}})/\overline{g_{\text{max}}}$ for both the elastic (dashed lines) and in-

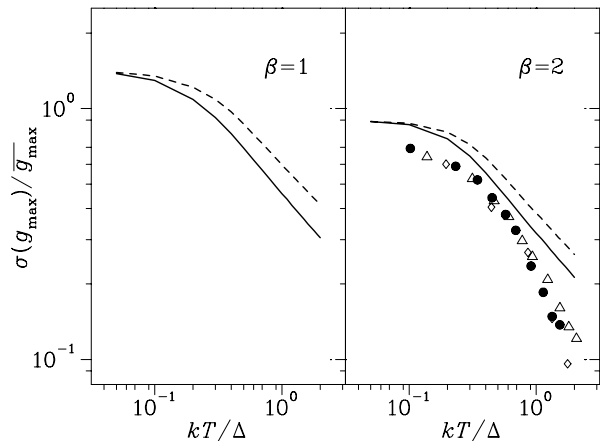


FIG. 3: The ratio $\sigma(g_{\max})/\overline{g_{\max}}$ between the standard deviation and average value of the peak height versus temperature kT in the elastic (dashed lines) and inelastic (solid lines) limits for both GOE (left) and GUE (right) symmetries. The symbols in the right panel are the experimental data of Ref. [12].

elastic (solid lines) limits and for both conserved (left panel) and broken (right panel) time-reversal symmetry. The symbols in the right panel are the experimental results [12]. While inelastic scattering enhances the suppression of the ratio $\sigma(g_{\max})/\overline{g_{\max}}$ at finite temperature, it still cannot explain the experimental findings at the present stage. We note, however, that even at low temperatures there is a discrepancy between the experimental data and the analytically known value for one-level conduction ($\sigma(g_{\max})/\overline{g_{\max}} = 2\sqrt{5}/5 \approx 0.8944$ for $\beta = 2$). As a probe of inelastic scattering, the parameters α and γ turn out to be far more sensitive than the ratio between the standard deviation and mean value. The increases of both the mean and the standard deviation of the peak height due to inelastic scattering, as seen in the right panels of Fig. 1, cancel out to a large extent in the quantity $\sigma(g_{\max})/\overline{g_{\max}}$, resulting in a reduced sensitivity of the latter to the inelastic scattering rate.

Conclusion. We have investigated the effect of inelastic

scattering inside the dot on the distribution of the conductance peak heights in the Coulomb-blockade regime. We found that the quantity γ measuring the decrease in the standard deviation of the conductance peak height upon breaking of time-reversal symmetry (relative to the value of the standard deviation for broken time-reversal symmetry) is sensitive to inelastic scattering of electrons within the dot. This quantity can serve as an independent experimental probe of inelastic scattering, in addition to the quantity α that was suggested and measured recently.

We thank C.M. Marcus for useful discussions. This work was supported in part by the U.S. DOE grant No. DE-FG-0291-ER-40608, and in part by the National Science Foundation under Grant No. PHY99-07949.

-
- [1] Y. Alhassid, Rev. Mod. Phys. **72** 895 (2000).
 - [2] A.G. Huibers, M. Switkes, C.M. Marcus, K. Campman, and A.C. Gossard, Phys. Rev. Lett. **81**, 200 (1998).
 - [3] A.G. Huibers, M. Switkes, C.M. Marcus, P.W. Brouwer, C.I. Duruöz, and J.S. Harris, Jr., Phys. Rev. Lett. **81**, 1917 (1998).
 - [4] U. Sivan, Y. Imry, and A.G. Aronov, Europhys. Lett. **28**, 115 (1994).
 - [5] B.L. Altshuler, Y. Gefen, A. Kamenev, and L. S. Levitov, Phys. Rev. Lett. **78**, 2803 (1997).
 - [6] R.A. Jalabert, A.D. Stone, and Y. Alhassid, Phys. Rev. Lett. **68**, 3468 (1992).
 - [7] Y. Alhassid, Phys. Rev. B **58**, R13383 (1998).
 - [8] J. A. Folk, C. M. Marcus, and J. S. Harris, Jr., Phys. Rev. Lett. **87**, 206802 (2001).
 - [9] C. W. J. Beenakker, Phys. Rev. B **44**, 1646 (1991).
 - [10] C. W. J. Beenakker, H. Schomerus, and P. G. Silvestrov, Phys. Rev. B **64**, 033307 (2001).
 - [11] E. Eisenberg, K. Held, and B. L. Altshuler, arXiv:cond-mat/0110609.
 - [12] S. R. Patel, D. R. Stewart, C. M. Marcus, M. Gökçedağ, Y. Alhassid, A. D. Stone, C. I. Duruöz, and J. S. Harris, Jr., Phys. Rev. Lett. **81**, 5900 (1998).
 - [13] Y. Alhassid, M. Gökçedağ, and A. D. Stone, Phys. Rev. B **58**, R7524 (1998).